Available online at www.sciencedirect.com

ScienceDirect

Energy Procedia 126 (201709) 1147–1154

Energy Procedia

www.elsevier.com/locate/procedia

72nd Conference of the Italian Thermal Machines Engineering Association, ATI2017, 6-8 September 2017, Lecce, Italy

A computational model of axial piston swashplate pumps

F. Fornarelli[a], A. Lippolis[a], P. Oresta[a], A. Posa[b] *

[a]*Dipartimento di Meccanica, Matematica e Management – Politecnico di Bari*
[b]*Marine Technology Research Institute – Italian National Research Council (CNR-INSEAN), Roma*

Abstract

Variable displacement hydraulic machines offer a very promising alternative and energy saving solution for many applications in mobile machines, mobile robots and other applications. In the present paper an axial piston swashplate pump will be theoretically analyzed and explained using the software AMESim in order to estimate the piston friction force and volumetric efficiency loss without hardworking experimental tests. The present paper is aimed at analyzing the forces acting on the swash plate in stationary and non-stationary conditions, in order to optimize the main design parameters of the control actuators of a variable displacement pump. The behavior of the machine is analyzed and presented at different angular velocities and pressure regimes.

Peer-review under responsibility of the scientific committee of the 72nd Conference of the Italian Thermal Machines Engineering Association

Keywords: Axial piston pump, Swash plate behaviour, Performance optimization.

1. INTRODUCTION

Since 50s several manufacturers have developed swash plate control axial piston pumps and several authors tried to propose accurate models of performance for hydraulic piston machines, which are especially appreciated for the high power density ratio. In 1981 Zarotti and Nervegna [1] introduced non-linear terms for force and flow losses. Several works due to Hooke (see, for instance, [2]) are focused on the study of the slippers connecting the piston to

* Corresponding author. Antonio Lippolis Tel.: +39 0994733317; fax: +0-000-000-0000
E-mail address: lippolis@poliba.it

1876-6102
Peer-review under responsibility of the scientific committee of the 72nd Conference of the Italian Thermal Machines Engineering Association
10.1016/j.egypro.2017.08.314

the swash plate. Ivantysynova investigated extensively axial pistons swashplate pumps [3] and especially the problem of the control of the swash plate [4]. Manring [5] analyzed carefully the force components moving the slipper away from the swash plate. The work by Heon and Hyoung [6] discussed in detail the force losses in such class of pumps. Roccatello et al. [7] adopted the AMESim software to simulate an axial piston pump. More recent works by Borghi et al. [8] e [9] are focused on the analysis of the motion of the slippers over the swash plate and on the critical condition causing the slipper to move away from the swashplate, respectively.
However, unfortunately so far there are no exhaustive models able to accurately describe the behavior of swash plate axial piston pumps throughout the whole operating range, i.e., at different rotational speeds, different delivery pressures and especially different displacement volumes. Furthermore, in almost all cases available literature focuses very accurately on specific details. For instance, Authors dealing carefully with mechanical details of the problem, utilize simplified approaches to handle volumetric losses and viceversa. In the present paper a new model, developed using AMESim software, is proposed. Our target in the present paper is to report a comprehensive computational tool, involving some simplifications, but accurate enough to help manufacturers in designing new axial piston pumps. Section 2 describes the geometry of the pump analyzed here and section 3 presents its theoretical analysis. In section 4 the model developed using AMESim software is shortly presented. Sections 5 and 6, respectively, discuss the volumetric and torque losses. Finally, in section 7 charts of pump performance are presented.

Nomenclature

A	surface of viscous friction	Q_{tr}	leakages flow rate
a	piston axial acceleration	R	piston radius
D	rotating body theoretical diameter	r	radial coordinate from cylinder axis
d	piston diameter	t	time variable
F_{ac}	frictional forces associated to centrifugal forces	V_p	piston axial velocity
F_p	pressure force on the piston	V_{tr}	lubricating oil velocity
F_μ	viscous friction forces	y	vertical piston position
f_a	static friction coefficient	z	piston axial position
g	cylinder/piston clearance	**Greek**	
L	piston/cylinder interference in axial direction	α	swash plate inclination
M_p	piston mass	θ	piston angular position
N	number of pistons	θ_0	angular gap between pistons
n	pump rotational speed	μ	dynamic viscosity
p	oil pressure inside cylinders	ρ	oil density
Q_m	delivery flow rate	ω	pump angular speed

2. PUMP GEOMETRY

The simulation model reported here is general. Nonetheless, in order to provide details about the geometry of the pump analyzed in the present paper, Fig. 1 shows pictures of some pump elements: the rotating body, the distribution plate, a piston and a slipper connecting the piston to the swash plate. The rotating body is composed of 9 cylinders accommodating the relative pistons. However in the present work simulations with different numbers of cylinders will be reported. The axes of the cylinders stand on a circumference of diameter D = 70 [mm], while the axial length of each cylinder is equal to 60 [mm]. All pistons, as well as the groove within each cylinder, have a diameter d = 17 [mm] and the clearance between them is equal to 200 [μm]; the axial length of all pistons is equal to 42 [mm]. As shown in Fig.1, each piston presents a spherical head with a diameter of 12 [mm], connected to the cylindrical body with a smooth fillet. The overall piston length, including its spherical head, is equal to 56 [mm]. The spherical head is coupled with the brass slipper in Fig. 1, which moves over the swash plate, keeping almost aligned with it. In contrast, the relative motion between the piston head and the slipper is over a sphere and is characterized by an amplitude depending on the effect of the friction forces. The main rotation of the slipper relative to the piston head is due to the rotation of the swash plate, affecting the actual pump displacement. In the present case it is a rotational motion on a plane around an axis parallel to that of rotation of the swash plate. The spherical

head is hollow and has a hole, aligned with the piston axis, which allows the oil within the cylinder to lubricate both the region between head and slipper and that between slipper and swash plate. The lubricating oil from the axial hole in the piston head goes into the leakage hole of the slipper, visible in the slipper on the side of the swash plate. Such oil generates a pressure level almost constant beneath the central circular groove with a height of 0.4 [mm] and a diameter of 11.5 [mm]. An outer circular crown with a diameter of 21 [mm] and in contact with the swash plate creates a very thin meatus causing significant losses and a conical evolution of pressure up to the pump body.

Fig. 1 – Pictures of the pump components

In Fig. 1 also the distribution plate is represented, connecting all cylinders with the suction and delivery channels. The distribution plate presents two port connection. The left one is composed of a single cavity, while the right one is divided in 5 holes, in order to increase the stiffness of the plate. The left port, connected with the suction channel, is characterized by a circumferential length of about 74 [mm], equivalent to 124°. Taking into account that the circumferential extent of each cylinder hole, coupled with the distribution plate, is equal to 17 [mm], that is 28°, each cylinder needs a rotation of 14°, after reaching the top dead centre, to be connected with the suction channel. The same applies for the bottom dead centre: each cylinder loses connection with the suction channel 14° before reaching such configuration. The 5 holes connected to the delivery channel have a circumferential length of 12 [mm] and a distance between each others of 4 [mm]. In such a case each cylinder needs a rotation of 13° in order to connect to the delivery channel from the bottom dead centre and the same rotation amplitude is required to each cylinder between losing connection with the delivery channel and reaching the top dead centre.

3. THEORETICAL ANALYSIS

The offset of the temporal scale was chosen in such a way the first piston at $t = 0$ is horizontal, therefore its angular position, relative to the horizontal direction, is defined as below:

$$\theta = 2\,\pi\,n\,t\,[rad] = 360\,\,n\,t\,[°] \tag{1}$$

where n is in [Hz] and t in [s]

All other pistons have angular positions with increments of:

$$\theta_0 = 2\,\pi / N\,[rad] = 360\,/ N\,[°] \tag{2}$$

The angular position allows us to compute the vertical position of each piston axis as:

$$y = D/2\,\sin\,(\theta) = D/2\,\sin\,(2\,\pi\,n\,t + \theta_0) \tag{3}$$

The axial position of each piston, depending on the inclination of the swash plate, ranging between 0° e 18°, is evaluated with reference to the rotation axis of the piston:

$$z = D/2\,\sin\,(\theta)\,\tan(\alpha) = D/2\,\tan(\alpha)\,\sin\,(2\,\pi\,n\,t + \theta_0) \tag{4}$$

First and second time derivatives provide velocity and acceleration for each piston:

$$V_p = \pi\,n\,D\,\tan(\alpha)\,\cos\,(2\,\pi\,n\,t + \theta_0) \tag{5}$$

$$a = -2\,\pi^2\,n^2\,D\,\tan(\alpha)\,\sin\,(2\,\pi\,n\,t + \theta_0) \tag{6}$$

Finally, flow-rate is given by the piston cross-section and velocity, while the force of each piston on the swash plate is given by the piston cross-section and the oil pressure:

$$Q_m = \pi\,\frac{d^2}{4}\,V_p \tag{7}$$

$$F_p = p\,\pi\,\frac{d^2}{4} \tag{8}$$

4. PUMP SIMULATION MODEL

Each piston presents the same behavior, therefore the AMESim model was developed only for one piston in a supercomponent. Thus, the entire pump consists of the assembly of a number of supercomponents equal to the number of pistons. In Fig.2 the scheme of a single supercomponent in the hypothesis of ideal conditions is presented, with oil compressibility, leakages and friction forces neglected. The icon 1 stands for the number of pistons *N*. The icons 2 and 3 give the output of the system, which are torque and flow-rate, respectively. The icon 4 stands for the angular velocity of the pump in [RPM]. The icon 5 represents the number of the analysed cylinder, in the range 0÷*N*-1. In fig.3 a scheme of a three pistons pump is reported, where each black icon represents one of the cylinders. The parameter in the top left area represents the angular velocity that is, indeed, constant for each cylinder. The parameter on the left bottom area represents the number of pistons, that is equal to 3 in this case. The only parameter linked to each supercomponent is the number of the corresponding cylinder. In particular, in this case it goes from 0 to 2. The first piston (0) has 0° phase shift, therefore cylinders 1 and 2 have 120° and 240° phase shift, respectively.

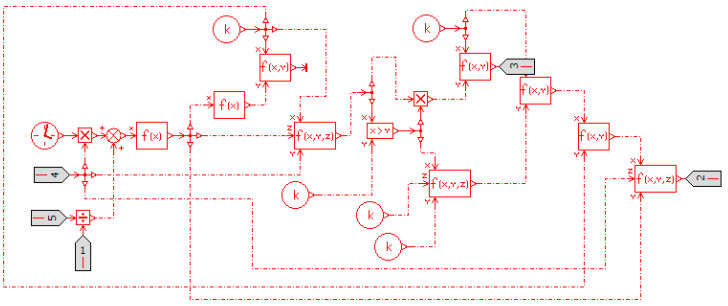

Fig. 2 – Ideal simulation model of a piston in AMESim.

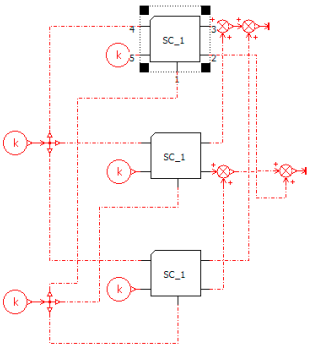

Fig. 3 – Model of a 3-pistons pump.

5. OIL COMPRESSIBILITY AND LEAKAGE LOSSES

The actual behavior of the pump differs from the ideal one because of the friction losses, compressibility of the oil and leakages. In this section the two latter effects are discussed, being the main ones influencing the volumetric efficiency of the pump.

At the beginning of the delivery stroke, the volume of the cylinder decreases, causing the increase of the oil pressure. This phenomenon is positive because the outlet pressure is very high, compared to the suction pressure and the pressure jump cannot be too abrupt. It is convenient also because of the design requirement to avoid a sharp passage from the suction to the outlet pressure and vice versa. The reduction of the flow rate due to the compressibility is just one of the causes. Another effect reducing the flow rate is the leakage due to the internal gaps. We can distinguish three main leakages: piston/cylinder, slipper/swash plate and distribution plate leakages. The leakage due to piston/cylinder clearance is caused by two main sources. One of them is the piston movement pushing the oil into the gap between piston and cylinder, which can be modelled by means of a linear velocity gradient, due to the small gap, equal to zero at the cylinder surface and equal to the piston velocity at the piston surface. The velocity is positive during the delivery phase, corresponding to the stroke from the bottom dead centre to the top dead centre, and negative during the suction phase. The second source of leakage is due to the pressure gradient through the gap between the internal and external regions of the cylinder. This effect is negligible during the suction phase, but it is important during the delivery phase, when the pressure gradient is maximum. It is possible to evaluate the flow rate associated to the linear velocity profile assuming a mean velocity equal to the piston mean velocity:

$$Q_{tr} = \frac{1}{2}\pi \; d \; g \; V_p \tag{9}$$

where g represents the gap between cylinder and piston, d is the cylinders diameter, V_p is the piston velocity, having a sinusoidal behavior from the bottom dead centre to the top dead centre and vice versa.

We have to take into account the parabolic profile associated to the pressure jump between internal and external regions of the cylinder. Due to the force balance along the axial direction of a hollow cylinder with thickness dr, considering the viscous forces on the lateral surfaces and the pressure forces on the top and bottom surfaces, we can state that:

$$\frac{\partial^2 V_{tr}}{\partial r^2} = \frac{\Delta p}{\mu \; L} \tag{10}$$

where μ is the dynamic viscosity, Δp is the pressure gap between the internal and external regions and L is the length of the lateral surface of contact between piston and cylinder. Integrating two times equation (10), we can find the flow rate equation:

$$Q_{tr} = -\frac{1}{12}\pi d g \frac{\Delta p \; g^2}{\mu \; L} \tag{11}$$

In the AMESim model the oil compressibility and the leakages are included as reported in fig. 4. The red part on the left is equal to that reported in fig.2 and is utilized to determine the position and the velocity of the piston. These data are the input of the right part of the model. The cylinder volume is simulated with an icon similar to a cylinder and the central sphere with a label Ch. The first element with a moving cylinder has a variable volume, whereas the sphere has a constant volume. The constant volume is about equal to the internal volume of the cylinder when the piston is at the top dead centre position. The variable volume models the cylinder stroke.

The central sphere is linked with other two spheres in order to take into account the inlet zone (the top sphere) and the outlet zone (the bottom sphere). The inlet zone was kept at 12 [bar] in all tests and was linked to the cylinder volume by means of a check valve allowing flow rate at suction, but not at delivery. Also a throttling valve is considered in order to model leakages. The pressure in the outlet zone is variable and here was chosen equal to 200 [bar]. The outlet region is connected to the cylinder volume by means of a check valve allowing the outlet, but avoiding the inlet during the suction phase. Downstream of the check valve there is a throttling valve to simulate the pressure losses through the distribution plate.

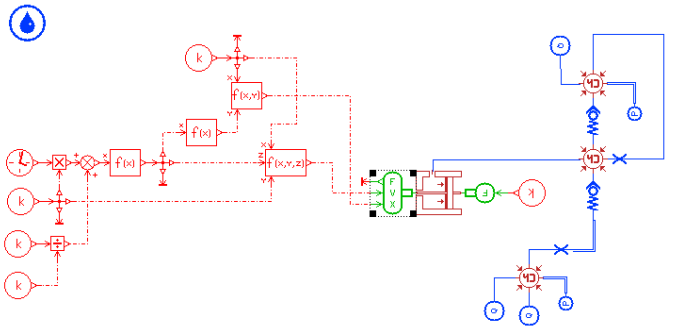

Fig. 4 – Simulation model in AMESim of a delivery piston.

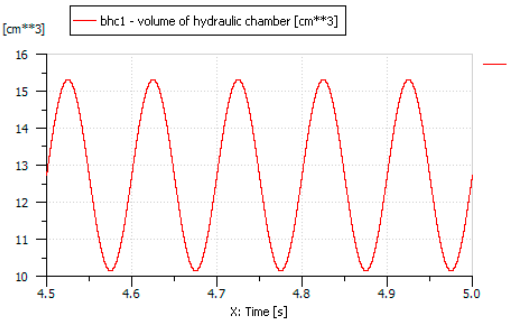

Fig. 5 – Cylinder volume performance, 0.5 [s]-5 Cycles.

In figure 5 the internal volume of the cylinder is shown, whose evolution is sinusoidal. In contrast, the inlet flow rate is not sinusoidal, as reported in figure 6: the detail of this effect is reported for just one cycle from the top dead centre to the bottom dead centre. The main source of this behavior is the cylinder pressure, keeping too high after the top dead centre to allow the suction phase to start. Thus for a period slightly smaller than 5 ms, corresponding to 18°, there is no suction. For 14° the cylinder is not in communication with the inlet, but this is not a problem because suction would not be possible. In figure 7 the outlet flow rate is provided (values are negative because outward from the cylinder). There, leakage effects are more important. Thus, for clarity, only leakages are reported in more detail in figure 8. Leakages are important during the outlet phase and reach 3% of the outlet flow rate. Leakages are almost constant, whereas the flow rate is dependent on the piston velocity. Pressure within the cylinder is rather low during the suction phase and instead high during the delivery phase, as reported in figure 9. We point

that the variation between the two values is not instantaneous, because of the oil compressibility. Such phenomenon is more obvious in figure 10, showing that oil compressibility causes a delay of 6 [ms], corresponding to 22° of pump rotation.

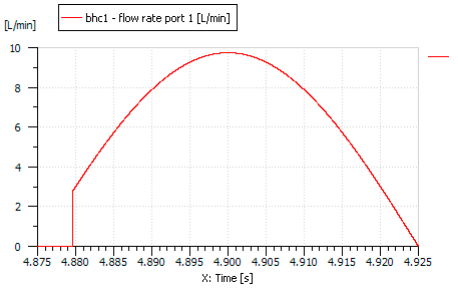

Fig. 6 – Suction flow performance between top and bottom dead points.

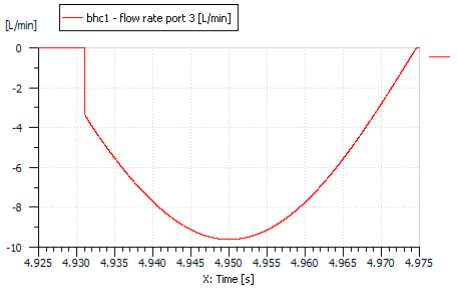

Fig. 7 – Delivery flow performance between bottom and top dead points.

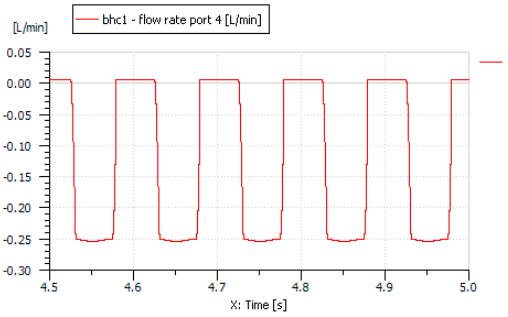

Fig. 8 – Flow loss performance, 0.5 [s]-5 Cycles

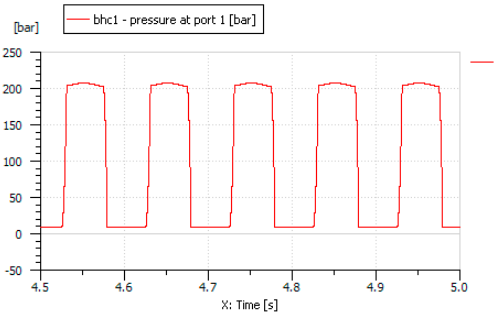

Fig. 9 – Cylinder pressure performance, 0.5 [s]-5 Cycles

6. MECHANICAL PERFORMANCE

The mechanical performance depends on several components, as below:

1) The oil pressure forces inside the cylinder;
2) The inertia forces;
3) The viscous friction forces;
4) The friction forces due to centrifugal force;
5) The viscous friction forces between the slipper and the swath plate.

The oil pressure forces were reported in equation (8).

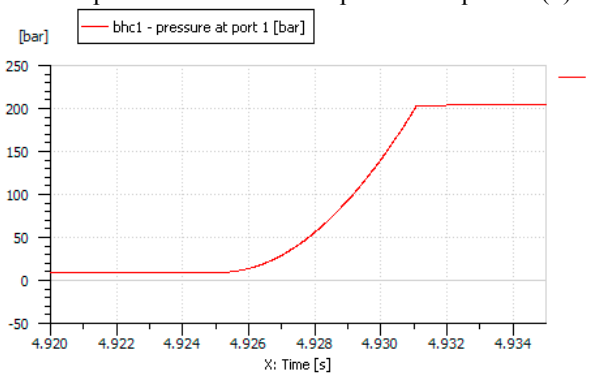

Fig. 10 – Pressure trend between suction and delivery phases.

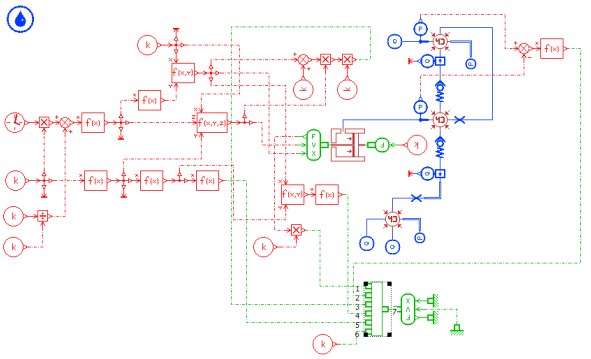

Fig. 11 – Simulation model in AMESim of a piston with friction losses and volumetric losses.

The inertia forces are calculated as the mass times the axial acceleration of the piston, where the overall mass is composed of the piston mass and the internal piston oil mass. The total mass was estimated to be approximately 70 [g].

The viscous friction force is the resistance of the oil flow on the piston and is proportional to the velocity derivative along the direction normal to the fluid motion. The fluid shear on the piston can be associated to two separate phenomena: the parabolic trend due to the pressure gradient and the linear trend due to the piston velocity. These phenomena were already presented in the last paragraph, equations (9)-(11). Using the overlapping effects principle, the viscous friction forces can been calculated as sum of two components.

The viscous friction force due to the pressure gradient is reported below:

$$F_{\mu 1} = \mu A \frac{\partial V_{tr}}{\partial n} = \mu \pi d L \frac{\Delta p}{2 \mu L} g = \pi d g \frac{\Delta p}{2} \tag{12}$$

In the final equation dynamic viscosity μ and length L do not appear.

The viscous friction force due to the piston speed is given by the equation below:

$$F_{\mu 2} = \mu A \frac{\partial V_{tr}}{\partial n} = \mu \pi d L \frac{V_p}{g} \tag{13}$$

Centrifugal force tends to push the piston outward. The centrifugal force is balanced by the cylinder reaction: all these forces act along the radial direction. The frictional forces in the axial direction, associated to the radial forces, are expressed by:

$$F_{ac} = f_a M_p \omega^2 R = f_a M_p (2\pi N)^2 R \tag{14}$$

Fig. 11 shows the full AMESim supercomponent, including both volumetric leakages and mechanical losses. All forces applied to the piston converge to the green element shown below. It is worth stressing the presence of pressure transducers, measuring both the pressure inside the cylinder and the pressure in the pump body.

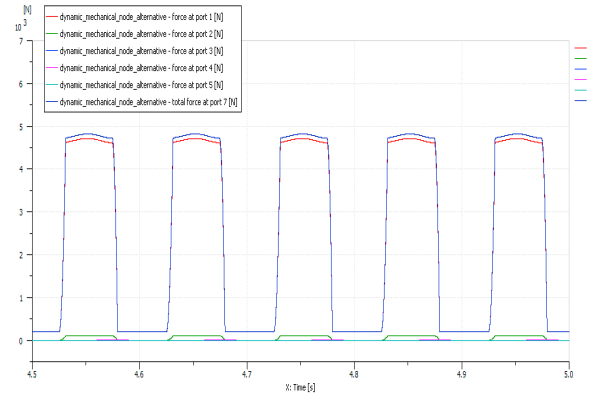

Fig. 12 – Piston axial force trend.

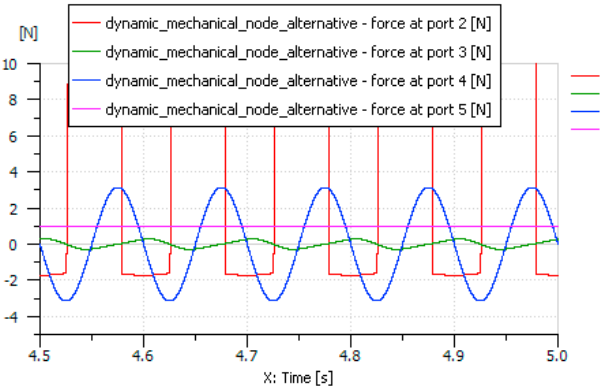

Fig. 13 – Secondary components of the piston axial force.

Fig. 12 shows the trends of all force components and their sum: the blue line, below in the caption, shows the total force. The red line is representative of the pressure force and the green line is representative of the viscous friction force due to the pressure gradient, while the other force components are obviously less significant. The other force components are shown enlarged in Fig. 13. The red line represents the viscous friction force due to the pressure gradient, already visible in Fig. 12. This force is reported during the suction phase, while the delivery phase is outside the figure range. The green line represents the viscous friction force due to the piston motion, whose evolution is strictly a sine-wave, as that of the piston speed. In figure this force is always less than 1 [N], but it should be noted that this loss is more important at high speeds, so at the maximum pump speed, 3000 [rpm], it would be 5 times higher. The blue line shows the inertia forces. It is worth noting that the inertia forces are proportional to the square of velocity and they do not contribute to the pump power. Indeed the energy accumulated during acceleration is returned during deceleration. The friction forces due to the centrifugal force are represented by the pink line. They are constant and approximately equal to 1 [N]. Also such forces are proportional to the square of the speed and would reach 25 [N] at the maximum pump speeds.

7. PUMP PERFORMANCE

The AMESim supercomponents allow computing pump performance as a function of pistons number, rotational speed and operating pressure. Fig. 14 shows the pump volumetric performance as function of rotational speed for three different values of operating pressure, 30, 150 and 300 [bar], respectively. The same pump volumetric performance is shown for three different rotational speeds, 300, 1500 and 3000 [RPM], respectively, in Fig. 15.

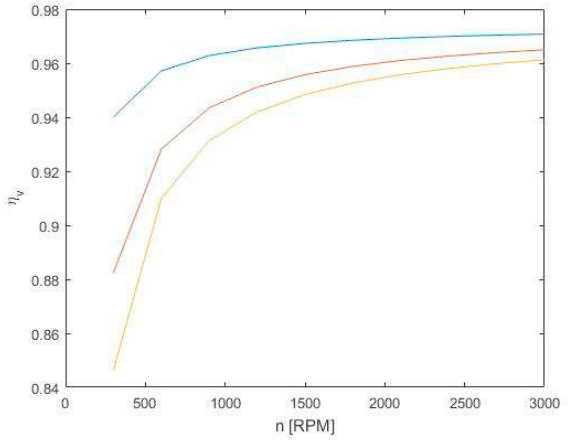

Fig. 14 – Volumetric efficiency diagram for 3 different pressure tests.

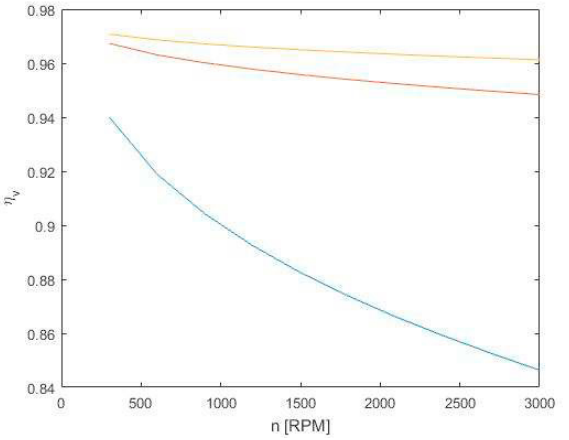

Fig. 15 – Volumetric efficiency diagram for 3 different speed tests.

8. SUMMARY

The present work analyzes the main phenomena affecting the volumetric and mechanical performance of a swash plate axial piston pump. Therefore, the methodology reported here can be considered a practical tool in order to reduce the considerable cost of testing before manufacturing. Nonetheless a final stage of comparison between simulations and experiments is still recommended before finalizing the new design.

REFERENCES

[1] Zarotti, G.L. and Nervegna, N. – "Pump efficiencies approximation and modelling" - Int Fluid Power Symp, 6th; Cambridge, Engl; 8-11 April 1981, Pages 145-164

[2] Koç, E. and Hooke, C.J. - "Investigation Into the Effects of Orifice Size, Offset and Overclamp Ratio on the Lubrication of Slipper Bearings", Tribology International, Elsevier Science, Vol. 29, No. 4, pp. 299 – 305, 1996.

[3] Ivantysyn, J. and Ivantysynova, M. – "Hydrostatic Pumps and Motors – Principles, Designs, Performance, Modelling, Analysis, Controll and Testing" – Academia Books International, New Delhi, 2000.

[4] Grabbel, J. and Ivantysynova, M. – "An investigation of swash plate control concepts for displacement controlled actuators" – International Journal of fluid Power, vol. 6, N. 2, pagg. 19-36, 2005.

[5] Manring, N. D., "Predicting the Required Slipper Hold-Down Force an Axial-Piston Swash Plate Type Hydrostatic Pump", Proc. of 2001 ASME Int. Mechanical Engineering Congr. and Exp., Novemb. 11-16, 2001, NY.

[6] Heon, S. J. and Hyoung, E. K. – "On the Istantanius and Average Piston Friction of Swash Plate Type Hydraulic Axial Piston Machines" - KSME International Journal, Vol. 18 No. 10, pp. 1700-1711, 2004

[7] Roccatello, A., Mancó, S., Nervegna, N. - "Modelling a variable displacement axial piston pump in a multibody simulation environment" – J. of Dynamic Systems, Measurement and Control, Trans. of the ASME, 129 (4), 2007.

[8] Borghi, M., Specchia, E., Zardin, B. - "Numerical Analysis of the Dynamic Behaviour of Axial Piston Pumps and Motors Slipper Bearings", 2009-01-1820, Accepted for Publication in the SAE 2009 International Powertrains, Fuels and Lubricants Meeting, June 15-17, 2009, Florence.

[9] Borghi, M., Specchia, E., Zardin, B., Corradini, E. - "The critical speed of slipper bearings in axial piston swash plate type pumps and motors" - (2010) Proc. of the ASME Dynamic Systems and Control Conf. 2009, DSCC2009.